U.S. DEPARTMENT OF THE INTERIOR
U.S. GEOLOGICAL SURVEY

THICKNESS OF CENOZOIC DEPOSITS AND LOCATION AND GEOMETRY OF THE LAS VEGAS VALLEY SHEAR ZONE, NEVADA, BASED ON GRAVITY, SEISMIC-REFLECTION, AND AEROMAGNETIC DATA

By

V.E. Langenheim[1], John Grow[2], John Miller[2], J.D. Davidson[1], and E. Robison[1]

Open-File Report 98-576

1998

---

[1]U.S. Geological Survey, MS 989, 345 Middlefield Rd., Menlo Park, CA 94025
[2]U.S. Geological Survey, MS 939, Box 25046, Denver Federal Center, Denver, CO 80225-0046

TABLE OF CONTENTS

TABLES

FIGURES

Abstract

The U.S. Geological Survey acquired detailed gravity data and a proprietary seismic-reflection profile in the northern part of the Las Vegas Valley to locate and characterize the Las Vegas Valley shear zone (LVVSZ) and the Las Vegas basin. Constraining the location and geometry of the LVVSZ is important for hydrologic flow models of the valley. The LVVSZ has offset and flexed in a right-lateral sense the predominantly north-south trending mountain ranges of southern Nevada. Its exact location and geometry are poorly known, but most workers infer that it passes beneath Las Vegas Valley. A steep northwest-trending gravity gradient marks the northern margin of the basin beneath Las Vegas Valley. Detailed gravity profiles indicate two breaks in slope along this gradient south and west of Gass Peak. The northernmost break in slope becomes more pronounced to the northwest towards Corn Creek Springs. The southernmost break in slope corresponds to the main basin edge and is 2-3 km south of basement exposures in the Las Vegas Range. This break in slope extends as far east as Frenchman Mountain. East of Frenchman Mountain the gravity gradient apparently steps over about 5 km to the south and coincides with the northern edge of a strongly magnetic block beneath Frenchman Mountain. A seismic-reflection profile sub-parallel and 1-3 km south of the gravity gradient indicates a 1-3-km-thick reflective package that is interpreted as Cenozoic sedimentary deposits. The thickness of Cenozoic deposits, based on an inversion of the gravity data constrained by borehole and seismic data, shows a narrow, deep basin north of Corn Creek Springs, that most likely formed by movement on the LVVSZ. The available gravity data suggest that the area between Corn Creek Springs and Las Vegas Valley is a local horst block between two prominent basins.

Introduction

The Las Vegas Valley Shear zone (LVVSZ) is a major Cenozoic structure that is responsible for the pronounced oroflexural bending of the mountain ranges north and south of Las Vegas Valley (Fig. 1). The shear zone offsets Paleozoic isopachs, structural trends, and facies boundaries in a right-lateral sense (Stewart and others, 1968). The shear zone appears to play a major role in the development of Las Vegas Valley (Plume, 1989; Campagna and Aydin, 1994; Langenheim and others, 1997) and may play a major role in the hydrology of the region. Despite these obvious effects of movement on the shear zone, its exact location beneath the basin fill of Las Vegas Valley is poorly known. For example, Longwell and others (1965) show the LVVSZ as a N60°W-trending fault extending from northeast of Frenchman Mountain to Indian Springs. Campagna and Aydin (1994) instead show the LVVSZ as several N70°W strands stepping across Las Vegas Valley to a point south of Frenchman Mountain (Fig. 2). Using water chemistry data, Lyles and Hess (1988) indicate that the shear zone trends more northerly (N40°W) across the valley and is 8-10 km wide ("Zone B" on Fig. 2). Langenheim and others (1997) use gravity and aeromagnetic data to locate and characterize the LVVSZ. Here we update that report by

incorporating newly acquired gravity and proprietary seismic-reflection data in the northern part of Las Vegas Valley. We determine the location of the shear zone by applying filters to both gravity and aeromagnetic data. We used a modified version of the iterative depth-to-basement calculation of Jachens and Moring (1990), incorporating picks on top of basement from seismic and well data, to provide information on the nature of the basins associated with the LVVSZ.

Acknowledgments

Many thanks to the Las Vegas Valley Water District for providing extensive support for this study. We are especially grateful to them for the access via helicopter to those rugged mountainous areas of the Spring Mountains, Sheep Range and Las Vegas Range. We also wish to thank Gary Dixon of the U.S. Geological Survey (USGS) for logistical support, Bruce Chuchel (USGS) for computer programming support, and William R. (Ric) Page and Tom Brocher (USGS) for reviews.

Previous Work on Las Vegas Valley Shear Zone

The Las Vegas Valley shear zone (LVVSZ) has offset the predominantly north-south trending mountain ranges of southern Nevada, bending them into large oroflexes (Fig. 1, 2). Mesozoic thrust faults are also offset right-laterally across the LVVSZ (Stewart and others, 1968). Longwell (1974) concluded that movement on the LVVSZ ended by the onset of deposition of the late Tertiary Muddy Creek Formation, as this unit is not cut by the shear zone. This observation and paleomagnetic (Sonder and others, 1994) and structural data (Duebendorfer and Black, 1992) bracket the principal period of movement along the LVVSZ between 14 and 8.5 Ma. Displacement along the shear zone probably decreases to the east (Salyards and Shoemaker, 1987) and the LVVSZ cannot be traced east of Hamblin Mountain (Fig. 2). The LVVSZ may be cut by the left-lateral Lake Mead fault system, although detailed mapping of Tertiary sedimentary facies indicates that the LVVSZ and the Lake Mead fault system were active simultaneously during at least part of the Miocene (Bohannon, 1984). Estimates of total displacement on the LVVSZ range from 23 to 69 km (Burchfiel, 1965; Stewart and others, 1968; Longwell, 1974; Wernicke and others, 1982); however, these estimates include as much as 44 km of additional bending.

The exact location of the LVVSZ is somewhat uncertain because it is concealed beneath thick alluvial deposits of Las Vegas Valley and has no surface expression. The best

available information on the location of the shear zone is based on gravity data. Plume (1989) noted the large gravity gradient along the northern margin of the valley and suggested that it may be caused by the LVVSZ. Using gravity data, Campagna and Aydin (1994) interpreted the LVVSZ as several N70°W strands stepping across Las Vegas Valley to a point south of Frenchman Mountain (Fig. 2). They argued that the LVVSZ is responsible for creating deep (>1 km) pull-apart basins beneath Las Vegas Valley. Langenheim and others (1997) also used gravity data to infer the location of the LVVSZ; they used the maximum horizontal gravity gradient to locate probable strands of the shear zone. Another source of information used to infer the location of the shear zone is water chemistry. Lyles and Hess (1988) used isotope and ion geochemistry of groundwater to delineate the LVVSZ; they indicate the shear zone trending N40°W across the valley; however, the distribution of well and spring data could also support the more traditional location of the LVVSZ of Longwell and others (1965).

Geologic Setting

For this study, basement rocks are defined as all pre-Cenozoic rocks and basin deposits are defined to be Cenozoic sedimentary and volcanic rocks. Basement rocks nearly ring Las Vegas Valley and are exposed in the Las Vegas and Desert Ranges, the Spring Mountains, and Frenchman Mountain (Fig. 2). The sequence exposed in the Spring Mountains consists of more than 7 km (23,000 ft) of Proterozoic and Paleozoic sedimentary rocks and approximately 1.2 km (4,000 ft) of Mesozoic sedimentary rocks (Longwell and others, 1965). Precambrian metamorphic and/or igneous rocks are inferred to underlie the Spring Mountains (Blank, 1987) on the basis of the stratigraphic section exposed at Frenchman Mountain and on the basis of the large gravity and magnetic anomalies present over the mountain range (Fig. 3 and 4). The structure of the Spring Mountains is very complex but, broadly, consists of a series of east-vergent thrust faults, most probably of Mesozoic age, that are cut by Tertiary block faulting (Longwell and others, 1965; Burchfiel and others, 1974).

In Las Vegas Valley, basin fill consists of Tertiary and Quaternary sedimentary and volcanic rocks (Maxey and Jameson, 1948). Most of Las Vegas Valley is underlain by alluvial deposits; volcanic rocks are exposed only in the southern part of the valley (Fig. 2).

Volcanic rocks exposed in the River, McCullough, and Eldorado Mountains were erupted between 21 and 12 Ma (Fig. 2; Anderson, 1971; Weber and Smith, 1987). Cenozoic volcanic units consist of andesitic and latitic lava flows and flow breccias and impede ground water movement from the valley fill south and east of Las Vegas Valley

(Maxey and Jameson, 1948). Cenozoic sedimentary formations, such as the Muddy Creek and Horse Spring Formations, are generally well-consolidated and well-cemented and probably do not act as significant aquifers, although local interbedded gravel and sand lenses may be capable of transmitting sizable quantities of water, especially within the Muddy Creek Formation.

By far the most important aquifers in the Las Vegas Valley fill reside within Pliocene and younger alluvial deposits. According to Maxey and Jameson (1948), faults offsetting these sediments are important barriers to ground water movement, although some of these faults may have acted as conduits for groundwater movement because of their association with spring deposits (Quade, 1986). Numerous faults are present within Las Vegas Valley (Bell, 1981), such as the Eglington and Whitney fault scarps (Fig. 2). The origin of the faults is somewhat controversial; they may be tectonic in origin or may be a response to compaction and subsidence within the basin due to groundwater withdrawal. The LVVSZ is a structure with many kilometers of offset and thus may have a profound effect on groundwater movement. Near Indian Springs, Winograd and Thordarson (1968) found a stair-stepped water table and attributed this to low permeability caused by the LVVSZ. Lyles and Hess (1988) instead argue that the LVVSZ in Las Vegas Valley forms a conduit or mixing zone based on groundwater chemistry.

Gravity and Aeromagnetic Data

645 gravity stations were collected with LaCoste & Romberg gravity meters G-17C and G-177 during August and November 1997 and May 1998 to supplement regional gravity coverage (Fig. 3; Kane and others, 1979; Langenheim and Jachens, 1996; Langenheim and Schmidt, 1996; Langenheim and others, 1997) and provide additional data over the LVVSZ. Gravity stations are non-uniformly distributed in the area (Fig. 3). Station spacing in Las Vegas Valley is on average 1-2 stations per km^2; in the mountainous regions, the station spacing is poorer and can be as low as 1 station per 10 km^2. We used a helicopter to access the rugged areas bordering the LVVSZ, obtaining 35 gravity stations. The data were tied to a base station, LVGS, established in front of the U.S. Geological Survey office in Las Vegas. LVGS (latitude 36°4.02'N; longitude 115°8.41'W) has an observed gravity value of 979593.62 mGal based on ties to CPA, a gravity base station that is part of the Mt. Charleston calibration loop (Ponce and Oliver, 1981; observed gravity value of 979522.22 mGal).

Gravity data were reduced using the Geodetic Reference System of 1967 (International Union of Geodesy and Geophysics, 1971) and referenced to the International Gravity

Standardization Net 1971 gravity datum (Morelli, 1974, p. 18). Gravity data were reduced to Bouguer anomalies using a reduction density of 2.67 g/cm^3. This includes corrections for earth-tide, instrument drift, elevation, latitude, and terrain. An additional isostatic correction using a sea-level crustal thickness of 25 km (16 miles), a crustal density of 2.67 g/cm^3, and a mantle-crust density contrast of 0.40 g/cm^3 was applied to the gravity data to remove long-wavelength gravitational effects of isostatic compensation of the crust due to topographic loading.

Horizontal control on the gravity station locations was provided by both surveying and by Trimble Global Positioning System (GPS) and Rockwell PGLR (Precision Lightweight GPS Receiver) receivers. Gravity station elevations along two of the detailed profiles were surveyed using an electronic-distance-measurement instrument. The elevations of gravity stations along the other detailed profiles were obtained using GPS. Other elevations were taken from benchmarks, spot elevations or interpolated from contours on the U.S. Geological Survey 7-1/2 minute topographic series maps. The uncertainty in the elevations of the surveyed stations is less than 0.3 m (1 ft), corresponding to an error of less than 0.06 mGal in the gravity values.

Terrain corrections were computed to a radial distance of 167 km and involved a three-part process: (1) Hayford-Bowie zones A and B with an outer radius of 68 m were estimated in the field with the aid of tables and charts, (2) Hayford-Bowie zones C and D with an outer radius of 590 m were computed using 30-m digital elevation models, and (3) terrain corrections from a distance of 0.59 km to 167 km were calculated using a digital elevation model and a procedure by Plouff (1977). Total terrain corrections for the stations collected for this study ranged from 0.2 to 32.7 mGal, averaging 2.0 mGal. If the error resulting from the terrain correction is considered to be 5 to 10% of the total terrain correction, the largest error expected for the data is 3.3 mGal. However, the average error resulting from the terrain correction for the area of interest is small (0.2 mGal).

Aeromagnetic data used to create Figure 4 consist of east-west flightlines from two separate surveys (U.S. Geological Survey, 1979, 1983). Both surveys were flown at 300 m (1000 ft) above ground along flightlines spaced 1.6 km (1 mile) apart. The data were adjusted to a common datum and then merged by smooth interpolation across a buffer zone along the survey boundaries (Saltus and Ponce, 1988).

To help delineate trends and gradients in the gravity field, we used a computer algorithm to locate the maximum horizontal gravity gradient (Blakely and Simpson, 1986; Fig. 5). Gradient maxima occur directly over vertical or near-vertical contacts that separate rocks of contrasting densities. We also calculated magnetization boundaries (Fig. 5) in the following way: First, in order to emphasize the edges of shallow magnetic sources, we

filtered the aeromagnetic data by subtracting the upward continuation of the aeromagnetic field from the actual data. Upward continuation is the transformation of aeromagnetic data measured on one suface to a higher surface; this operation tends to smooth the data by attenuation of short-wavelength anomalies (Blakely, 1995). We upward continued the data 100 m. Subtraction of the upward-continued field from the original data results in high-pass filtered, residual anomalies, thereby accentuating shallow sources. Second, the residual aeromagnetic field was mathematically transformed into pseudogravity anomalies (Baranov, 1957); this procedure effectively converts the magnetic field to the "gravity" field that would be produced if all the magnetic material were replaced by proportionately dense material. Third, the horizontal gradient of the pseudogravity field was calculated everywhere by numerical differentiation. Lastly, locations of the locally steepest horizontal gradient were determined by numerically searching for maxima in the horizontal gradient grid (Blakely and Simpson, 1986).

Seismic-Reflection Data

The U.S. Geological Survey reprocessed nearly 40 km of multi-channel seismic-reflection data along line LV-4 (Figure 6A). The profile was purchased from Seitel, Inc. with limited publication rights. It was originally acquired by Pacific West Exploration Co., in the fall of 1978. Figures 6B and 6C show the corresponding potential-field data along the profile. The seismic-reflection data were acquired for three reasons: (1) to obtain independent data on the thickness of Cenozoic fill as constraints for the gravity inversion, (2) to calculate the density of the basin fill from seismic velocities, and (3) to image the structure of the basin fill. Unfortunately, the profile does not cross the pronounced gravity gradient interpreted as the LVVSZ along the northern margin of the valley, but parallels the gradient (Fig. 3). Fortunately, the profile is located at the base of the gravity gradient and therefore should provide useful information on the thickness of the Cenozoic fill in the deep part of the basin.

The seismic data were recorded at a nominal subsurface coverage of 24-fold using 48 recording channels, geophone group interval of 67 m, 2 ms sample interval and 6 s record length. The energy source was 61 m of primacord explosive buried at 30 inches (76 cm) depth. The energy point source interval was 67 m. Reflected energy was typically rich in frequencies between 8 to 50 Hz.

The data were reprocessed by us using a crooked line geometry scheme and a processing flow which consisted of automatic gain control, 2-window spiking deconvolution, 2 passes of velocity analyses and 2 passes of surface consistent residual statics calculations. The data were migrated after stacking using a time- and space-varying

velocity field, derived by smoothing the final stacking velocities. Typical near-surface interval velocities used for migration were 2.4 km/s and velocities increased to approximately 6.0 km/s at a two way travel time (TWTT) of 2.5 s. The migrated data were then converted to depth using the same interval velocity field as that used for migration.

The velocities used for the depth conversion provide constraints on the densities of the underlying rocks. Using the relationship of Gardner and others (1974) developed for sedimentary rocks,

$$\rho=0.23v^{0.25}$$

one can estimate the density, ρ (g/cm^3), from the sonic interval velocity, v (ft/s; Table 1).

Table 1--Sonic velocities and corresponding densities

Depth (in TWTT)	Sonic velocity range	Average Velocity	Average Density	Density Range (+/- 10%)*
0-400 ms	2.1-2.4 km/s	2.1 km/s	2.10 g/cm^3	2.05-2.15 g/cm^3
400-900 ms	2.4-4.3 km/s	3.4 km/s	2.36 g/cm^3	2.12-2.41 g/cm^3
900-2500 ms	4.3-5.5 km/s	4.6 km/s	2.55 g/cm^3	2.43-2.61 g/cm^3
> 2500 ms	6.0 km/s	6.0 km/s	2.72 g/cm^3	

* calculated using 10% uncertainty on the average velocity.

The smoothed interval velocities for LV-4 are 2.1-2.4 km/s (7000-8000 ft/s) for the upper 400 ms. A strong velocity gradient of 2.4-4.3 km/s (8000 to 14000 ft/s) exists from about 400 to 900 ms. Velocities then increase gradually to 5.5 km/s (18000 ft/s). It is difficult to assess the uncertainties in these interval velocities because of the lack of well logs and check shots. The error is probably +/- 10%, but could be as high as +/- 20%. Velocities are poorly constrained beneath 2.0 s (approximately 3 km). For comparison, sonic velocities measured on Cenozoic sedimentary rocks in the Mobil Virgin River 1A well (about 100 km northeast of Frenchman Mountain) are 2.1-3.0 km/s (7000-10000 ft/s) for the first second TWTT, increasing to 5.5 km/s (18000 ft/s) at about 2 seconds TWTT (Bohannon and others, 1993).

The upper 1-2 seconds TWTT of the data show a reflective package for the western 2/3 of the profile (Fig. 6A). The reflective package is about 1 second thick at shotpoint 1011 and extends at least as far east as shotpoint 1419, where the base of the package is approximately at 2 s TWTT. Between shotpoints 1419 and 1467, the reflections change character and are difficult to trace farther east. The change in reflective character coincides with a large gravity gradient (Fig. 6B) and the western margin of an aeromagnetic low (Fig. 6C). The low is part of the aeromagnetic high-low pair generated by the edge of the magnetic block underlying Frenchman Mountain (Fig. 4). Beneath the reflective package

is a series of discontinuous reflections that extend to 4 seconds TWTT between shotpoints 1200 and 1400. Many of these reflectors, such as those at 2 s TWTT and shotpoint 1165, have a southeast dip and have a dip steeper than the overlying reflectors. Some of these deeper reflections, however, are multiples of the reflections in the upper package (e.g., below shotpoint 1419). Sandwiched between the upper reflective package and the southeast-dipping reflectors is an area characterized by poor or scattered reflections. This relatively non-reflective package is thin or non-existent at the western end of the profile and thickens to the east below shotpoints 1317-1368.

We have picked three separate horizons on the LV-4 depth section (Figure 7). Layer 1a is composed of horizontal or gently dipping reflections in the upper 1 second TWTT. Layer 1b is separated by layer 1a by an unconformity, an angular unconformity most notably developed near shotpoint 1350 (22.6 km). The base of layer 1b is not a sharp discontinuity and is defined as the absence of coherent, continuous reflections. Layer 1c is composed of the southeast-dipping reflections that appear to flatten at about shotpoint 1270. Layers 1a and 1b thicken to the southeast to about shotpoint 1200. East of shotpoint 1450, however, reflections of the upper two layers lose coherency. The transition from the coherent reflections northwest of shotpoint 1450 to the package of reflections southeast of shotpoint 1504 could be an overlapping of Cenozoic deposits onto basement or a fault zone. The seismic and gravity data cannot distinguish between these two possibilities. We have interpreted this break as a fault at shotpoint 1450 (Fig. 7) because this portion of the profile crosses a structurally complicated junction of the LVVSZ and the northeast-trending fault bounding the west side of Frenchman Mountain. Both regional gravity and aeromagnetic data (Figures 3 and 4) indicate that the LVVSZ is not 2-dimensional in this area and that the seismic profile may cross a right stepover in the LVVSZ (Langenheim and others, 1997). The fault at shotpoint 1450 could either be associated with the stepover in the LVVSZ or a continuation of the northeast-trending fault bounding Frenchman Mountain.

We interpret the reflective layers 1a and layer 1b to be Cenozoic deposits. The disrupted, discontinuous nature of the layer 1c reflections may reflect (a) pre-Cenozoic rocks deformed by either Mesozoic thrust faulting or movement on the LVVSZ at depth, (b) the presence of non-reflective Mesozoic rocks, or (c) non-reflective Cenozoic coarse-grained or poorly-stratified sedimentary rocks deposited during the formation of the Las Vegas Valley basin. Mesozoic thrust faults do project from the north and south into LV-4 (Fig. 2). Seismic-reflection profiles and a sonic velocity log from the Virgin River depression (100 km northeast of Frenchman Mountain) indicate that the upper part of the Mesozoic section has very low reflectivity (Bohannon and others, 1993). Alternatively,

layer 1c could be Cenozoic deposits disrupted by movement on the shear zone. However, the velocity estimate for layer 1c is about 5.5 km/s, approximately the average velocity for Paleozoic rocks in the Virgin Valley well and much higher than the average sonic velocity measured for equivalent Cenozoic sedimentary rocks to the north (2.5 to 3.0 km/s; Bohannon and others, 1993). We prefer the interpretation that layer 1c is pre-Cenozoic.

At several places along the profile the fairly continuous reflections of layers 1a and 1b are disrupted by small faults. These faults have small vertical displacements (less than 200 ms; Fig. 7). These faults may have also some lateral movement, especially if they are associated with LVVSZ; however, the seismic data cannot constrain the existence or amount of lateral movement. One of the more prominent faults imaged on the profile is at shotpoint 1250; this location is approximately on strike with the Eglington fault scarp. Unfortunately the data in the upper 400 ms do not indicate whether the offset can be traced closer to the surface and it is difficult to ascertain the amount of offset on the pre-Cenozoic basement surface. The southeast-vergent anticline at shotpoint 1350 also appears to be disrupted by small faults. The anticline is also approximately on strike with a cluster of northeast-trending Quaternary faults about 7 km east of the Eglington fault. This anticline appears to deform layers 1b and 1c, but does not affect layer 1a. Because we believe layer 1b to be Cenozoic, this anticline is most likely not associated with Mesozoic thrust deformation, but could be formed by movement on the LVVSZ. The age of the base of layer 1a would then constrain the end of significant motion on the shear zone.

Drill Hole Data and Physical Properties

Although many boreholes have been drilled in Las Vegas Valley, only a handful have penetrated pre-Cenozoic rock. Lintz (1957) and Longwell and others (1965) present limited drill log information for some of these boreholes. Plume (1989) shows the locations of boreholes that bottom in both pre-Cenozoic rock and alluvial deposits, but does not present stratigraphic information for the individual boreholes. Water wells in the western part of the valley give minimum thicknesses of 240-300 m of alluvium (Maxey and Jameson, 1948; Las Vegas Valley Water District logs, written commun., 1996).

Table 2 summarizes density measurements of rock hand samples from the area. This table includes 26 new rock property measurements from the Spring and the McCullough Mountains. Densities of Cenozoic volcanic rocks range from 2.27 to 2.61 g/cm^3 (Langenheim and Schmidt, 1996; this study). Pre-Cenozoic basement densities vary from 2.21 (Mesozoic gypsum-rich beds) to 2.94 g/cm^3 (Precambrian gneiss). Mesozoic

sedimentary rocks have an average density of 2.50 g/cm^3; Paleozoic sedimentary rocks have an average density of 2.68 g/cm^3.

Little information is available on the density of the alluvial deposits of Las Vegas Valley. The average density of the Cenozoic sedimentary rocks in Table 2 does not accurately reflect the overall density of the alluvial deposits because it is strongly influenced by measurements of calcrete. Calcrete probably does not contribute a large volume to the alluvial deposits, but it is more easily sampled than the unconsolidated materials in the valley. One drill hole in Las Vegas Valley (78E on Fig. 2) provides information on porosity of the alluvial deposits (Las Vegas Valley Water District, written commun., 1996; Langenheim and Jachens, 1996). Well logs from this borehole indicate that the upper 174 m (570 ft) of alluvium (primarily gravel and sand) has an average porosity of 23%. Below 174 m, the alluvium has an average porosity of 15%. Using the equations in Langenheim and Jachens (1996), the density of the alluvial deposits (as derived from the porosity data) is 2.08 and 2.30 g/cm^3, assuming that all the clasts have a density of 2.7 g/cm^3 and that the deposits are not saturated. If all the pores are filled with water, the bulk densities would be 2.31 and 2.45 g/cm^3, respectively. These densities are comparable with densities calculated from the velocity data (Table 3).

Magnetic susceptibility data were also collected on hand samples. The sedimentary rocks of all ages are essentially nonmagnetic (Table 2). Susceptibilities of Precambrian schist exposed along the western edge of Frenchman Mountain range from 0.25 to 2.85 x 10^{-3} cgs units. Volcanic rocks exposed south of Las Vegas Valley are characterized by variable susceptibilites, ranging from 0.00 to 4.40 x 10^{-3} cgs units (Langenheim and Schmidt, 1996; this study). We do not have remanent magnetization measurements for these samples, but we suspect that remanent magnetization could be a significant contribution to the total magnetization of some of the volcanic rocks exposed south of Las Vegas Valley.

Gravity and Aeromagnetic Anomalies of the LVVSZ

The northern strand of the LVVSZ as described by Campagna and Aydin (1994) coincides approximately with the northwest-trending gravity gradient marking the northern edge of the Las Vegas Valley gravity low (Fig. 3). The steep gradient south of Gass Peak (GP) is at least 30 km long. We collected additional detailed gravity profiles across this steep gradient at its western and eastern ends (Fig. 3; Fig. 8). Profiles B, C and D all show a west-facing gravity gradient. The magnitude of the gradient decreases from nearly 9 mGal on Profile D to only 4 mGal on Profile B. Superimposed on the west-facing

gradient are two steps. The steps coincide with linear density boundaries (Fig. 5) that extend to the southeast. The eastern step is associated with a local gravity low, which becomes more distinct to the northwest. Detailed profiles 1 and 2 (on Fig. 8 map) indicated two steps along the gradient (Langenheim and others, 1997). Profile E, to the east, does not, but shows a smooth decrease in gravity values (Fig. 8E). 2-1/2-dimensional modeling along profiles 1 and C suggests that the northern density boundary reflects the edge of a local thickening of basin sediments (Fig. 9). The modeling confirms that the southern maxima (Fig. 5) mark the abrupt thickening of basin fill (Fig. 9).

The steep gravity gradient associated with the northern margin of the Las Vegas Valley decreases in magnitude towards Corn Creek Springs. The magnitude of the gradient is greatly diminished along Profile C (Fig. 8), however, a local break in slope in the gravity does occur. More gravity data are needed between Corn Creek Springs and this profile in order to constrain the configuration of the gravity gradients in this area; however, the available data suggest that at least two strands of the LVVSZ exist in this area. Corn Creek Springs is located on the extreme southeast corner of a narrow (> 10 km wide), elongated gravity low that extends 20 km northwestward to Indian Springs (Fig. 3). The southwestern margin of the low is marked by a steep gravity gradient, clearly delineated on Figure 5. The gradient is roughly on trend with the northwest projection of the southern density boundary associated with the northern margin of Las Vegas Valley basin. The northeastern margin of the Corn Creek Springs low is also marked by a gravity gradient, albeit less steep. The northeastern gradient coincides approximately with the Corn Creek Spring fault(s), that have documented late Quaternary movement (Haynes, 1967; Quade, 1986). This gradient may also reflect another strand of the LVVSZ. The available gravity data do not indicate either of these gravity gradients extending west of Indian Springs.

The southeastern terminus of the steep gravity gradient along the northern margin of Las Vegas Valley appears to bend sharply to the southwest, on trend with the continuation of the northeast-trending gradient associated with the eastern edge of the Las Vegas Valley gravity low (Fig. 3). The bend in the gradient also roughly coincides with the contact between alluvial deposits and Muddy Creek Formation (Longwell and others, 1965). A northwest-trending gravity gradient does continue eastward beyond the bend towards Gale Hills (Fig. 3). It has the same trend as the northern edge of the Las Vegas Valley low, but is stepped over to the south by about 5 km, along a line that parallels the northern margin of Frenchman Mountain. The polarity of the gradient has also changed from south-facing to north-facing.

The aeromagnetic data show a broad low (Fig. 4) paralleling the trend of the LVVSZ as defined by the gravity gradient. The automatically determined edge of the sources of the

magnetic highs over the Spring Mountains and Las Vegas Valley is at least 10 km south of the inferred location of the LVVSZ based on gravity (Fig. 5). The lack of a magnetic signature of the LVVSZ across Las Vegas Valley is not surprising because the alluvial deposits of the basin and the Paleozoic sedimentary sequence exposed north of the LVVSZ are at most weakly magnetic. A weak magnetization boundary nonetheless does coincide with the location of the steep gravity gradient south of Gass Peak (Fig. 5). However, caution should be exercised in interpreting this boundary because the east-west survey flightlines cross the LVVSZ at a highly oblique angle, and the filtering process may have produced artifacts in the residual data.

North of Frenchman Mountain, the aeromagnetic data indicate a strong west-northwest-trending magnetization boundary (Fig. 5). The intense aeromagnetic high over Frenchman Mountain appears to be truncated and elongated by a structure parallel to the LVVSZ (Fig. 4). The magnetization boundary also coincides quite closely (within 1 km) with a pronounced density boundary. The flightline direction makes it difficult to assess whether this magnetization boundary coincides exactly with the density boundary along the northern boundary of Frenchman Mountain.

Langenheim and others (1997) created 2 1/2 dimensional models using the program HYPERMAG (Saltus and Blakely, 1993) along a north-south tieline (Profile A-A'; Fig. 4) to ascertain the geometry of this boundary. The models indicate that the northern edge of the density and magnetic source of the Frenchman Mountain block boundary is approximately in the same place. The modeling shows that the top of the magnetic source is very shallow (< 1 km) and that the northern edge of the magnetic source is vertical. Exposed Paleozoic and Mesozoic rocks do not account for the aeromagnetic high. The most likely source for the anomaly is Precambrian crystalline rocks, which are locally exposed on the western margin of Frenchman Mountain (Longwell and others, 1965). Measurements indicate that these rocks are very magnetic (Table 2).

Depth to Basement

Method

We also calculated the depth to basement to determine the configuration of the basins beneath Las Vegas Valley. The method used in this study to estimate the thickness of Cenozoic rocks is an updated version of the iterative method developed by Jachens and Moring (1990) that incorporates drill hole and other geophysical data (Bruce Chuchel, U.S. Geological Survey, written commun., 1996). The method requires knowledge of the residual gravity field, of the exposed geology, and of the vertical density variation within the Cenozoic basin deposits. Data from drill holes that penetrate basement rock and

geophysical data that provide constraints on the thickness of the basin fill can also be input into the model and provide useful constraints to the method as well as a test of the results. The method attempts to separate the gravity field into two components, that which is caused by variations of density within the pre-Cenozoic basement and that which is caused by variations of thickness of the Cenozoic basin fill. To accomplish this process, the gravity data are separated into observations made on basement outcrops and observations made on Cenozoic deposits. The second set of observations is inverted to yield the thickness of Cenozoic deposits, based on an estimate of the density-depth function that characterizes the Cenozoic deposits. The inversion is complicated by two factors: (1) basement gravity stations are influenced by the gravity anomaly caused by low-density deposits in nearby basins, and (2) the basement gravity field varies laterally because of density variations within the basement. The inversion presented here does not take into account lateral variations in the density distribution of the Cenozoic deposits.

To overcome these difficulties, a first approximation of the basement gravity field is determined by interpolating a smooth surface through all gravity values measured on basement outcrops. Basement gravity values are also calculated at locations where drill holes penetrated basement or other geophysical data constrain the basement surface, using the Cenozoic density-depth function. The basin gravity is then the difference between the observed gravity field on the original map and the first approximation of the basement gravity field and is used to calculate the first approximation of the thickness of Cenozoic deposits. The thickness is forced to zero where basement rock is exposed. This first approximation of the basement gravity is too low near the basin edges because of the effects of the nearby low-density deposits on the basement stations. The basement gravity station values are "corrected" for the effects of the low-density deposits (the effects are calculated directly from the first approximation of the thickness of the Cenozoic deposits) and a second approximation of the basement gravity field is made by interpolating a smooth surface through the corrected basement gravity observations. This iteration leads to an improved estimate of the basin gravity field, an improved depth to basement and a new correction to the basement gravity values. This procedure is repeated until successive iterations produce no significant changes in the basement gravity field.

Results

We created basin models using density-depth functions derived from borehole porosity data and seismic velocities (Table 3) and using two different picks on the top of basement (the base of layer 1b versus the base of layer 1c) from LV-4. All the models we created utilize basement gravity stations and all available well data that constrain the thickness of

Cenozoic fill. Regardless of the choice of density-depth function or seismic basement picks, the basement gravity field produced by the models (Fig. 10) indicates high basement gravity values over Frenchman Mountain and Saddle Island where Precambrian rocks are exposed. Low basement gravity values coincide with exposures of Mesozoic sedimentary rocks (e.g. Gale Hills and area southwest of Lone Mountain). Only in the area of Corn Creek Springs and the area north of Frenchman Mountain do the basement gravity contours parallel the LVVSZ. Langenheim and Jachens (1997) correlated the basement gravity low over Lone Mountain with the basement gravity low over Gale Hills to estimate a maximum of 40 km of right-lateral offset along the LVVSZ.

Figure 11 shows the basin configurations for the end-member models A and B. The average difference between the thickness of sediments from well data or inferred from seismic data and the calculated thicknesses is 13.7 meters for model A (assuming that the basement surface is the base of layer 1b and the well-derived density-depth function). The average difference for model B (assuming the base of layer 1c is the basement contact and the seismically-derived density-depth function) is slightly higher, 15.6 meters. The resulting distribution of basin sediments (Fig. 11), regardless of the density-depth function or seismic picks, indicates the deepest part of the basin is 5 km west of Frenchman Mountain and reaches thicknesses of more than 4 km. This deep subbasin trends northeast, parallel to mapped scarps of the Frenchman Mountain fault system (Bell, 1981). The subbasin also has a part that trends northwest towards the center of the valley and parallels the gravity gradient along the southwest margin of Frenchman Mountain. The seismic picks on basement confirm that the basement gravity high associated with Frenchman Mountain extends west into the valley (Fig 10). 2-1/2-dimensional modeling of gravity data along LV-4 (Fig. 12) also confirms higher-density basement rocks beneath the eastern part of the Las Vegas Valley. The estimate of the thickness of basin fill in this area is strongly affected by the magnitude of the basement gravity high. Using the base of layer 1c leads to an even greater basement gravity high and therefore greater thickness of basin fill. We prefer model A (Fig. 11) because (1) it fits the actual control points slightly better and (2) seismic velocities suggest that layer 1c is the pre-Cenozoic basement.

The character of the basin north of Corn Creek Springs is quite different from the basin configuration beneath Las Vegas Valley. Using the 1-km contour line as a guide, the Corn Creek Springs basin is very narrow, no more than 5 km wide, and elongated. Its morphology suggests a pull-apart origin (Campagna and Aydin, 1994). In contrast to the Corn Creek Springs basin, the basin beneath Las Vegas Valley is at least 10 km wide and consists of at least three somewhat elongated sub-basins with N70°W, N50°W, and N40°E strikes. This difference in basin morphology suggests that the basin beneath Las

Vegas Valley may have had a more complicated structural history than the Corn Creek Springs basin. With the existing data, we cannot rule out the presence of a series of strike-slip faults stepping across Las Vegas Valley as inferred by Campagna and Aydin (1994; Fig. 2); in fact, the deep, northwest-trending subbasin west of Frenchman Mountain (Fig. 11) may be evidence for strike-slip motion under this part of the valley. However, the northeast-trending subbasin immediately west of Frenchman Mountain suggests that right-lateral strike-slip motion may not be the only mechanism for the formation of the Las Vegas valley basin. Part of the basin may have formed by high-angle normal faulting prior to movement on the LVVSZ.

Recommendations

Additional drill hole data and a better density-depth function would allow us to greatly refine the current models of the Las Vegas Valley basin. Because our models are constrained only by basement gravity stations and spatially limited well and seismic data, the basement gravity field over Las Vegas Valley cannot resolve basement gravity anomalies that have wavelengths less than the spacing between basement outcrops with gravity observations and wells and seismic control points (as much as 10 km across Las Vegas Valley). Drill hole data, particularly those wells that provide depths to basement rocks, could greatly improve the resolution of the basement gravity field. Additional geophysical data, such as seismic reflection or refraction or electrical data, would also provide much needed, independent constraints on basin thickness. A seismic-reflection profile perpendicular to LV-4 would provide better information on the geometry and nature of the LVVSZ, especially if coupled with a deep well with sonic and density information. Electrical data may address whether the LVVSZ is a conduit for ground water in addition to providing potential information on the depth and extent of aquifers. The density-depth function could be improved by borehole gravity surveys in existing boreholes.

References

Anderson, R.E., 1971, Thin skin distension in Tertiary rocks of southeastern Nevada: Geological Society of America Bulletin, v. 82, p. 42-58.

Baranov, V.I., 1957, A new method for interpretation of aeromagnetic maps: Pseudo-gravimetric anomalies: Geophysics, v. 22, p. 359-383.

Bell, J.W., 1981, Subsidence in Las Vegas Valley: Nevada Bureau of Mines and Geology Bulletin 95, 84 p., 1 plate, scale 1:62,500.

Blakely, R.J., 1995, Potential Theory in Gravity and Magnetic Applications: Cambridge University Press, Cambridge, England, 441 p.

Blakely, R.J., and Simpson, R.W., 1986, Approximating edges of source bodies from magnetic or gravity anomalies: Geophysics, v. 51, p. 1494-1498.

Blank, H.R., 1987, Role of regional aeromagnetic and gravity data in mineral-resource investigations, southeastern Nevada *in* USGS Research on Mineral Resources—1987, Third Annual V.E. McKelvey Forum on Mineral and Energy Resources, U.S. Geological Survey Circular 995, p. 5-6.

Bohannon, R.G., 1984, Nonmarine sedimentary rocks of Tertiary age in the Lake Mead region, southeastern Nevada and northwest Arizona: U.S. Geological Survey Professional Paper 1254, 72 p.

Bohannon, R.G., Grow, J.A., Miller, J., and Blank, H.R., Jr., 1993, Seismic stratigraphy and tectonic development of Virgin River depression and associated basins, southeastern Nevada and northwestern Arizona: Geological Society of American Bulletin v. 105, p. 501-520.

Burchfiel, B.C., 1965, Structural geology of the Specter Range quadrangle, Nevada and its regional significance: Geological Society of America Bulletin 76, p. 175-192.

Burchfiel, B.C., Fleck, R.J., Secor, T., Vincelette, R.R., and Davis, G.A., 1974, Geology of the Spring Mountains, Nevada: Geological Society of America Bulletin, v. 85, p. 1013-1022.

Campagna, D.J., and Aydin, Attila, 1994, Basin genesis associated with strike-slip faulting in the Basin and Range, southeastern Nevada: Tectonics, v. 13, no. 2, p. 327-341.

Duebendorfer, E.M., and Black, R.A., 1992, Kinematic role of transverse structures in continental extension: An example from the Las Vegas Valley shear zone, Nevada: Geology, v. 20, p. 1107-1110.

Gardner, G.H., Gardner, L.W., and Gregory, A.R., 1974, Formation velocity and density: the diagnostic basis for stratigraphic traps: Geophysics, v. 39, p. 770-780.

Haynes, C.V., 1967, Quaternary geology of the Tule Springs area, Clark County, Nevada, in Pleistocene Studies *in* Southern Nevada, Wormington, H.M, and Ellis, D., eds., Nevada State Museum of Anthropology Paper no. 13, p. 1-104.

International Union of Geodesy and Geophysics, 1971, Geodetic Reference System 1967: International Association of Geodesy Special Publication no. 3, 116 p.

Jachens, R.C., and Moring, B.C., 1990, Maps of the thickness of Cenozoic deposits and the isostatic residual gravity over basement for Nevada: U.S. Geological Survey Open-File Report 90-404, 15 p., 2 plates.

Kane, M.F., Healey, D.L., Peterson, D.L., Kaufmann, H.E., and Reidy, D., 1979, Bouguer gravity map of Nevada—Las Vegas sheet: Nevada Bureau of Mines and Geology Map 61, scale 1:250,000.

Langenheim, V.E., and Jachens, R.C., 1996, Thickness of Cenozoic deposits and groundwater storage capacity of the westernmost part of the Las Vegas Valley, inferred from gravity data: U.S. Geological Survey Open-File Report 96-259, 29 p.

Langenheim, V.E., and Jachens, R.C., in press, Structural framework of the Las Vegas Valley, Nevada, as determined by gravity and aeromagnetic data: Nevada Bureau of Mines and Geology Special Publication.

Langenheim, V.E., Jachens, R.C., and Schmidt, K.M., 1997, Preliminary location and geometry of the Las Vegas Valley Shear Zone, Nevada: U.S. Geological Survey Open-File Report 97-441, 25 p.

Langenheim, V.E., and Schmidt, K.M., 1996, Thickness and storage capacity of basin fill of the northern part of the Eldorado Valley, Nevada, and the extent of the Boulder City pluton: U.S. Geological Survey Open-File Report 96-512, 27 p.

Lintz, Joseph, Jr., 1957, Nevada oil and gas drilling data, 1906-1953: Nevada Bureau of Mines and Geology Bulletin 52, 80 p.

Longwell, C.R., 1974, Measure and date of movement on Las Vegas Valley shear zone, Clark County, Nevada: Geological Society of America Bulletin, v. 85, p. 985-990.

Longwell, C.R., Pampeyan, E.H., Bowyer, Ben, and Roberts, R.J., 1965, Geology and mineral deposits of Clark County, Nevada: Nevada Bureau of Mines and Geology Bulletin 62, 218 p.

Lyles, Brad E., and Hess, John W., 1988, Isotope and ion geochemistry in the vicinity of the Las Vegas Valley Shear Zone: Water Resources Center, Desert Research Institute, University of Nevada System Publication #41111, 78 p.

Maxey, G.B., and Jameson, C.H., 1948, Geology and water resources of Las Vegas, Pahrump, and Indian Spring valleys, Clark and Nye Counties, Nevada: State of Nevada Office of the Engineer Water Resources Bulletin no. 5, 121 p. (+43 p. appendix), 6 sheets.

Morelli, C.(Ed.), 1974, The International Gravity Standardization Net, 1971: International Association of Geodesy Special Publication no. 4, 194 p.

Plouff, Donald, 1977, Preliminary documentation for a FORTRAN program to compute gravity terrain corrections based on topography digitized on a geographic grid: U.S. Geological Survey Open-File Report 77-535, 45 p.

Plume, R.W., 1989, Ground-water conditions in Las Vegas Valley, Clark County, Nevada: U.S. Geological Survey Water-Supply Paper 2320-A, 15 p., 5 sheets.

Ponce, D.A., and Oliver, H.W., 1981, Charleston Peak gravity calibration loop, Nevada: U.S. Geological Survey Open-File Report 81-985, 20 p.

Quade, Jay, 1986, Late Quaternary environmental changes in the upper Las Vegas Valley, Nevada: Quaternary Research, v. 26, p. 340-357.

Saltus, R.W., and Blakely, R.J., 1993, HYPERMAG—An interactive 2- and 2 1/2-dimensional gravity and magnetic modeling program, Version 3.5: U.S. Geological Survey Open-File Report 93-287, 39 p.

Saltus, R.W., and Ponce, D.A., 1988, Aeromagnetic map of Nevada—Las Vegas sheet: Nevada Bureau of Mines and Geology Map 95, scale 1:250,000.

Salyards, S.L., and Shoemaker, E.M., 1987, Landslide and debris-flow deposits in the Thumb Member of the Miocene Horse Spring Formation on the east side of Frenchman Mountain, Nevada: A measure of basin-range extension: Geological Society of America Centennial Field Guide—Cordilleran section, p. 49-51.

Sonder, L.J., Jones, C.H., Salyards, S.L., and Murphy, K.M., 1994, Vertical axis rotations in the the Las Vegas Valley Shear Zone, southern Nevada: Paleomagnetic constraints on kinematics and dynamics of block rotations: Tectonics, v. 13, no. 4, 769-788.

Stewart, J.H., Albers, J.P., and Poole, F.G., 1968, Summary of regional evidence for right-lateral displacement in the western Great Basin: Geological Society of America Bulletin, v. 79, p. 1407-1414.

U.S. Geological Survey, 1979, Aeromagnetic map of southern Nevada: U.S. Geological Survey Open-File Report 79-1474, 1 sheet, scale 1:250,000.

U.S. Geological Survey, 1983, Aeromagnetic map of part of the Las Vegas 1° by 2° quadrangle, Nevada: U.S. Geological Survey Open-File Report 83-729, 1 sheet, scale 1:250,000.

Weber, M.E., and Smith, E.I., 1987, Structural and geochemical constraints on the reassembly of disrupted mid-Miocene volcanoes in the Lake Mead-Eldorado Valley area of southern Nevada: Geology, v. 15, no. 6, p. 553-6.

Wernicke, Brian, Spencer, J.E., Burchfiel, C.B., and Guth, P.L., 1982, Magnitude of crustal extension in the southern Great Basin: Geology, v. 10, no. 10, p. 499-502.

Winograd, I.J., and Thordarson, W., 1968, Structural control of ground-water movement in miogeosynclinal rocks of south-central Nevada *in* Eckel, E.B., editor, Nevada Test Site: Geological Society of America Memoir 110, p. 35-48.

Table 2. Densities, in g/cm^3 and susceptibilites (10^{-3} cgs units)

Precambrian crystalline rocks		Average	Susceptibility	
No. Samples	Density Range	Density	Range	Susceptibility
3	2.63-2.94	2.83	0.25-2.85	1.04
Mesozoic sedimentary rocks		Average	Susceptibility	
No. Samples	Density Range	Density	Range	Susceptibility
13	2.21-2.67	2.50	0.00-0.01	0.00
Paleozoic sedimentary rocks		Average	Susceptibility	
No. Samples	Density Range	Density	Range	Susceptibility
33	2.24-2.85	2.68	0.00-0.00	0.00
Cenozoic sedimentary rocks		Average	Susceptibility	
No. Samples	Density Range	Density	Range	Susceptibility
3	2.15-2.63	2.46	0.00-0.00	0.00
Cenozoic volcanic rocks		Average	Susceptibility	
No. Samples	Density Range	Density	Range	Susceptibility
17	2.27-2.61	2.47	0.00-4.40	0.60

Table 3. Density-depth functions*

Depth Range	Model (Based on well 78E**)		Seismic Depth Range	Seismic
	sediments	volcanics		sediments
0-200 m	-0.60	-0.45	0-500m	-0.60
200-600 m	-0.40	-0.40	500-1300 m	-0.35
>600 m	-0.25	-0.25	> 1300 m	-0.15

*density contrast in g/cm^3.

**Las Vegas Valley Water District, written commun., 1996; Figure 2

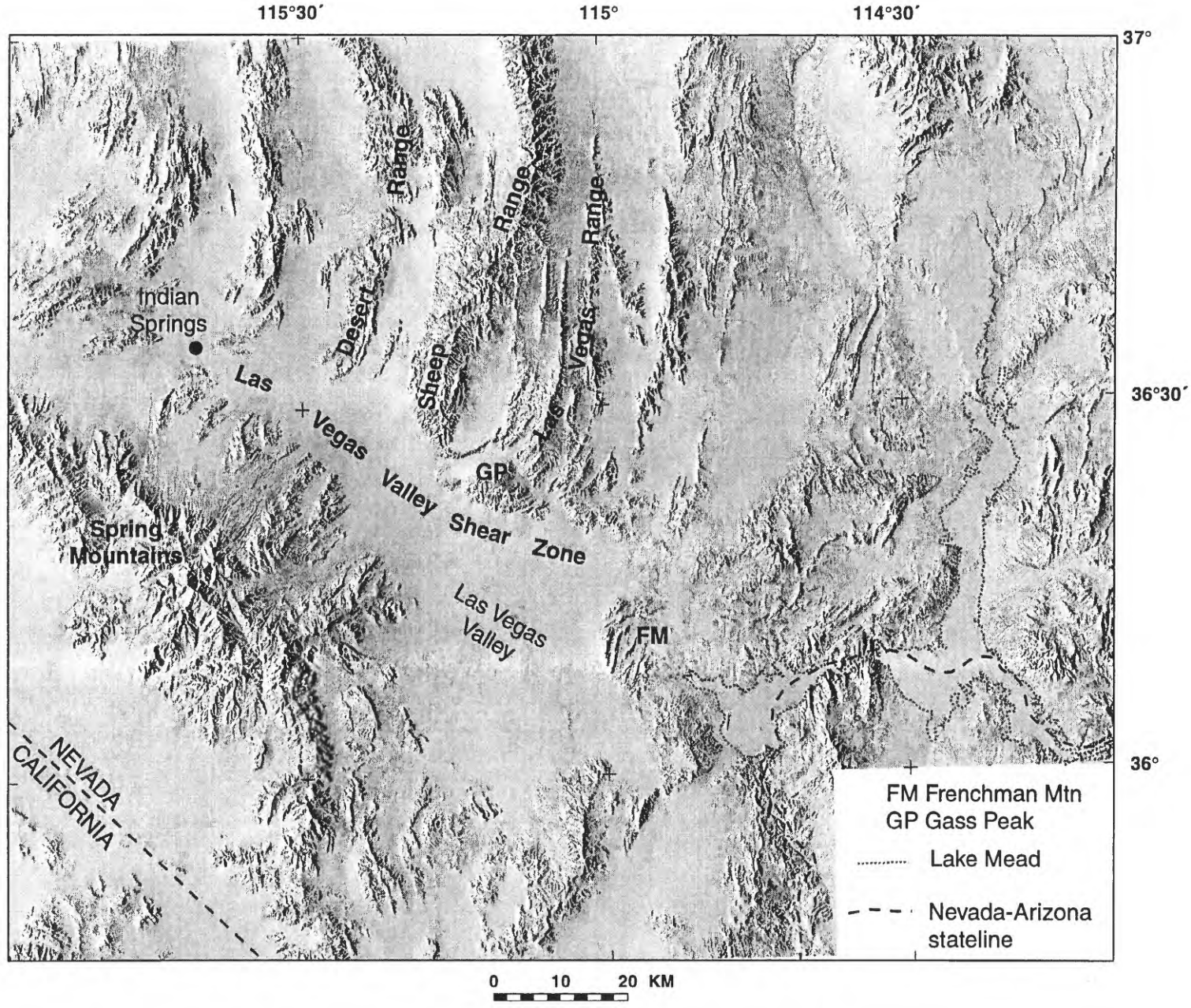

Figure 1. Shaded-relief topographic map of the study region.

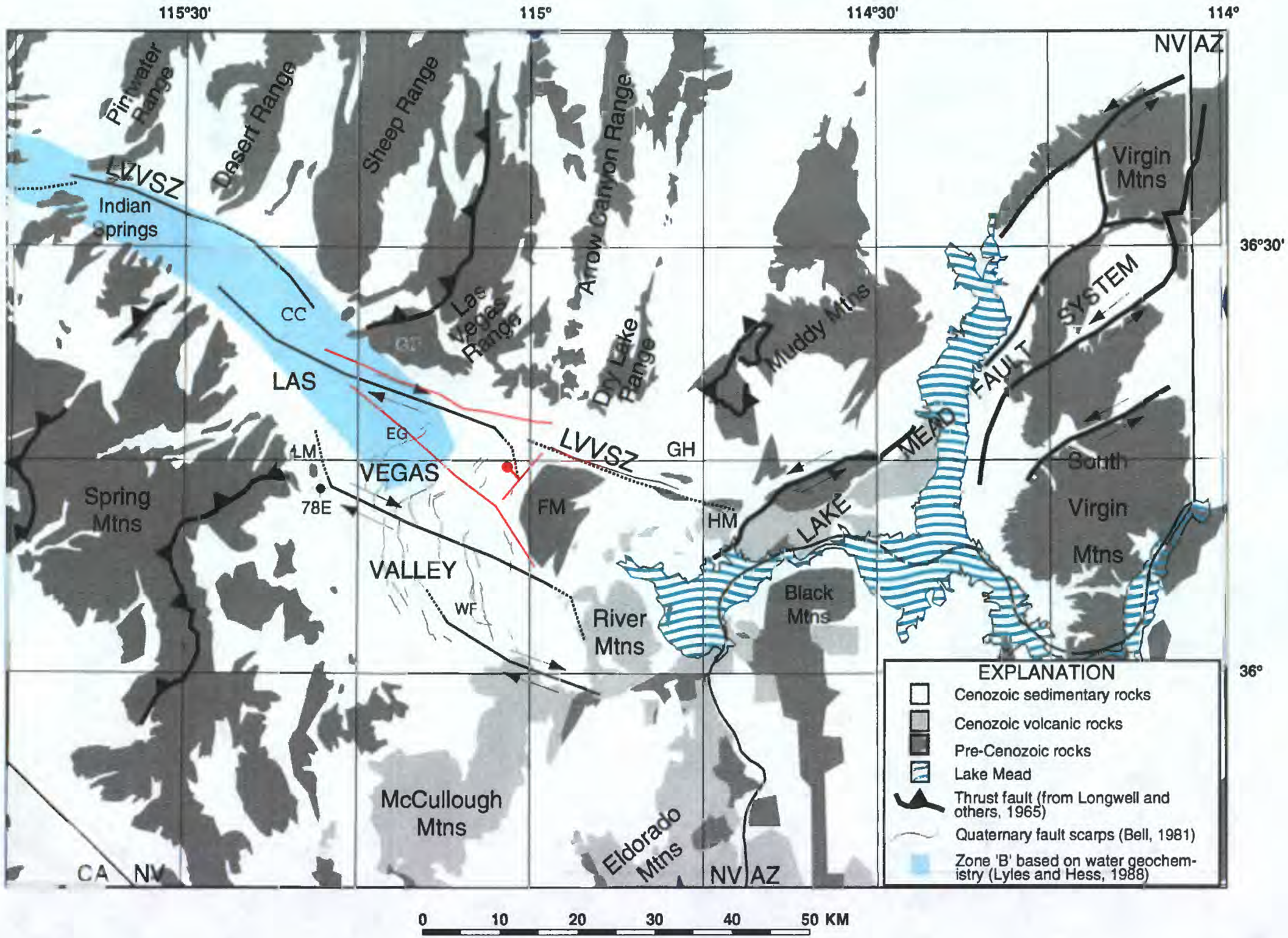

Figure 2. Simplified geologic map of the Las Vegas region showing the location of the Las Vegas Valley Shear Zone (LVVSZ) from Campagna and Aydin (1994). Most workers agree on the general location of the northern strands of the LVVSZ from Indian Springs to north of Frenchman Mountain (FM), but disagree the location of the LVVSZ south and west of FM. Geologic mapping does not indicate that the LVVSZ extends beyond Hamblin Mountain (HM). CC, Corn Creek Springs; EG, Eglington scarp; GH, Gale Hills; GP, Gass Peak; LM, Lone Mountain; SI, Saddle Island; WF, Whitney fault. Red lines indicates our preferred location of the LVVSZ and major fault on the western margin of Frenchman Mountain.

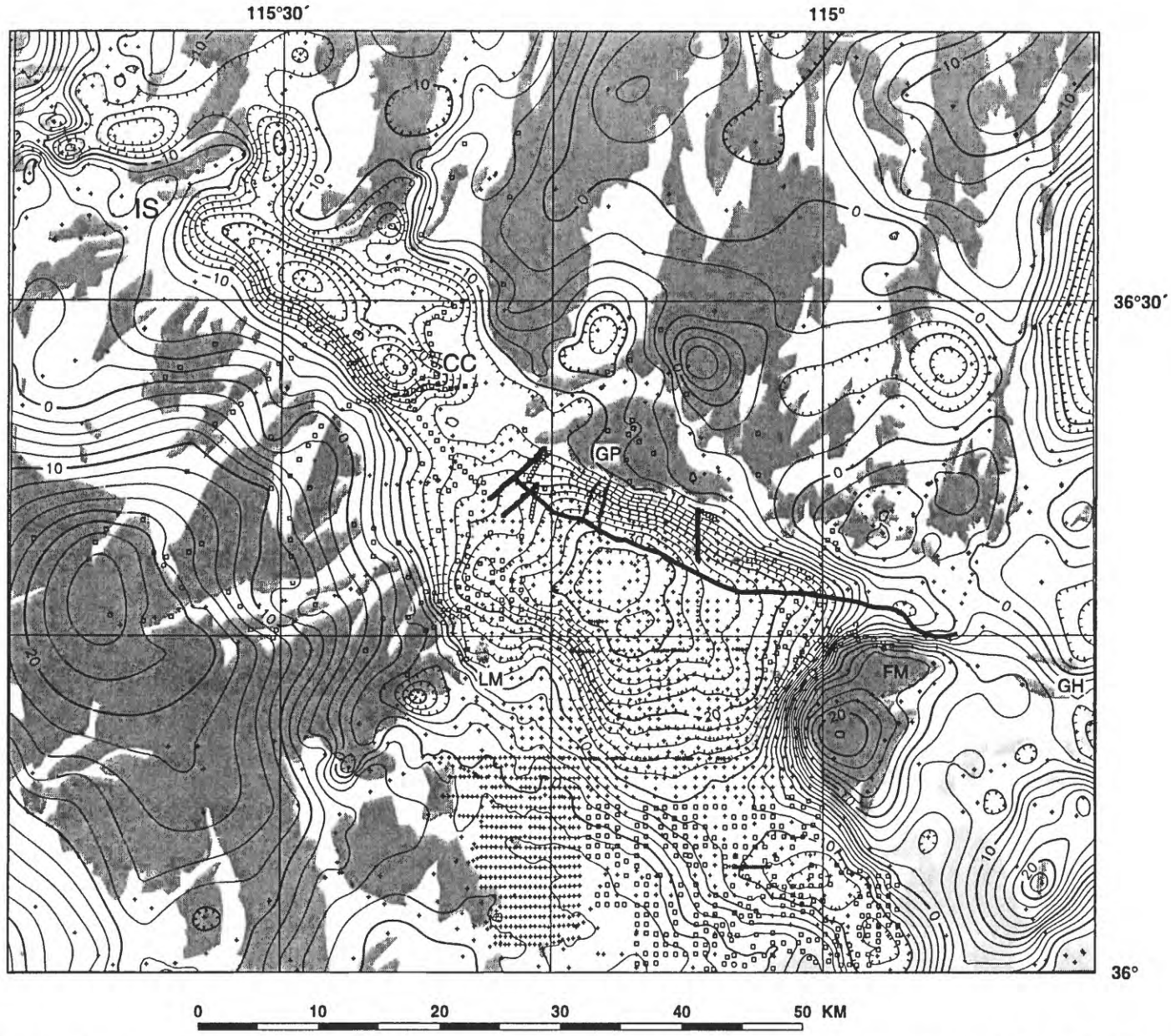

Figure 3. Isostatic gravity map of the Las Vegas Valley Shear Zone region. Contour interval, 2 mGal. See Figure 2 for explanation. Boxes, new gravity stations; crosses, previously collected stations. Sources of previously collected data are Kane and others (1979), Langenheim and Jachens (1996), Langenheim and Schmidt (1996), and Langenheim and others (1997). Northwest-trending thick black line indicates seismic profile LV-4. CC, Corn Creek Springs; FM, Frenchman Mountain; GH, Gale Hills; GP, Gass Peak; IS, Indian Springs; LM, Lone Mountain.

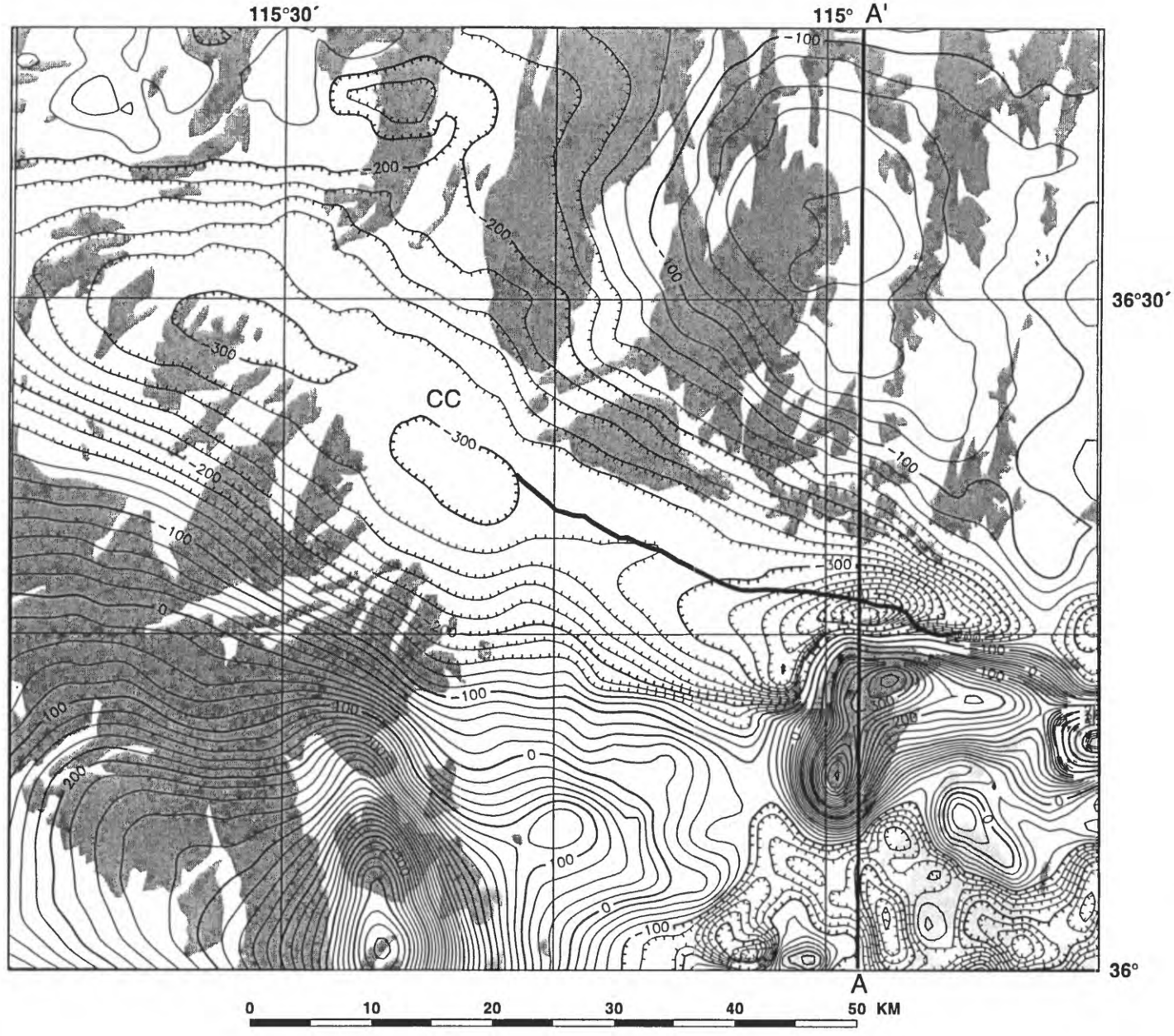

Figure 4. Aeromagnetic map of the Las Vegas Valley shear zone region. Contour interval, 20 nT. See Figure 2 for explanation of geology. Thick black line indicates seismic profile LV-4. CC, Corn Creek Springs.

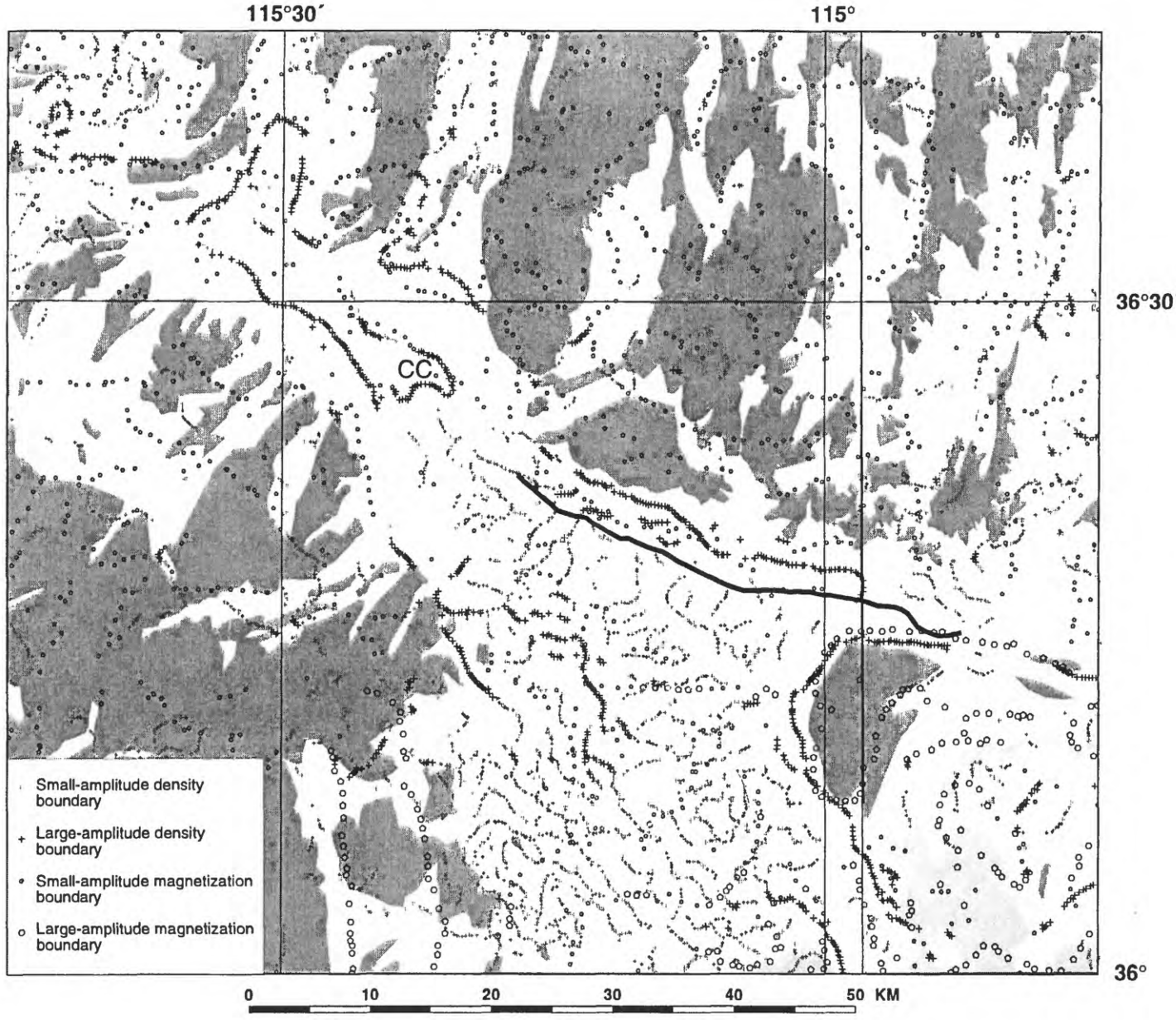

Figure 5. Density and magnetization boundaries in the Las Vegas Valley Shear zone region. Thick black line is seismic-reflection profile LV-4. CC, Corn Creek Springs.

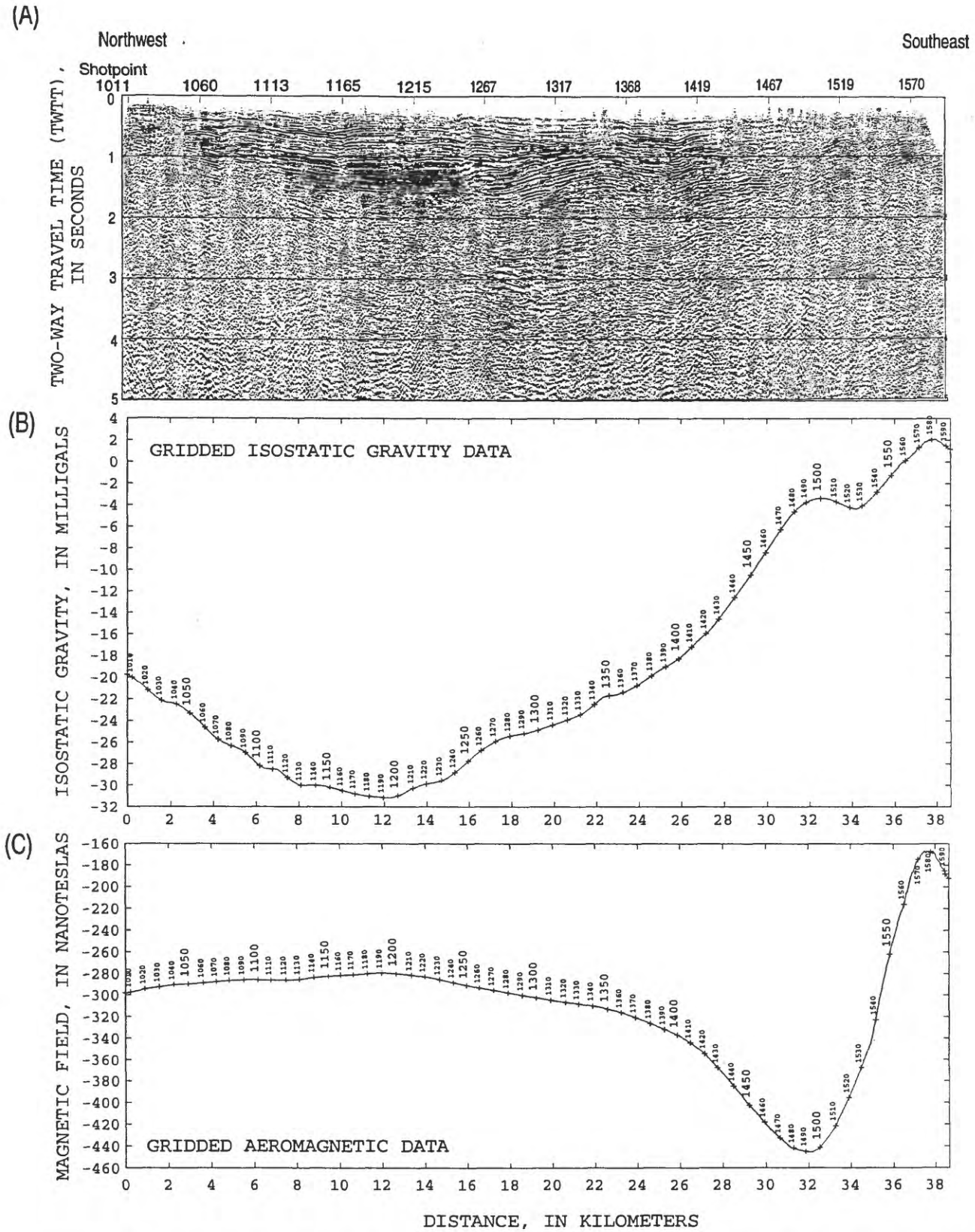

Figure 6. Data along seismic-reflection profile LV-4. (A) Migrated time section of seismic-reflection data; (B) isostatic gravity data and (C) aeromagnetic data. Profile begins at shotpoint 1006 and ends at shotpoint 1593. Numbers on (B) and (C) show shotpoint numbers along the profile. Datum is 2700 feet (823 m) above sea level.

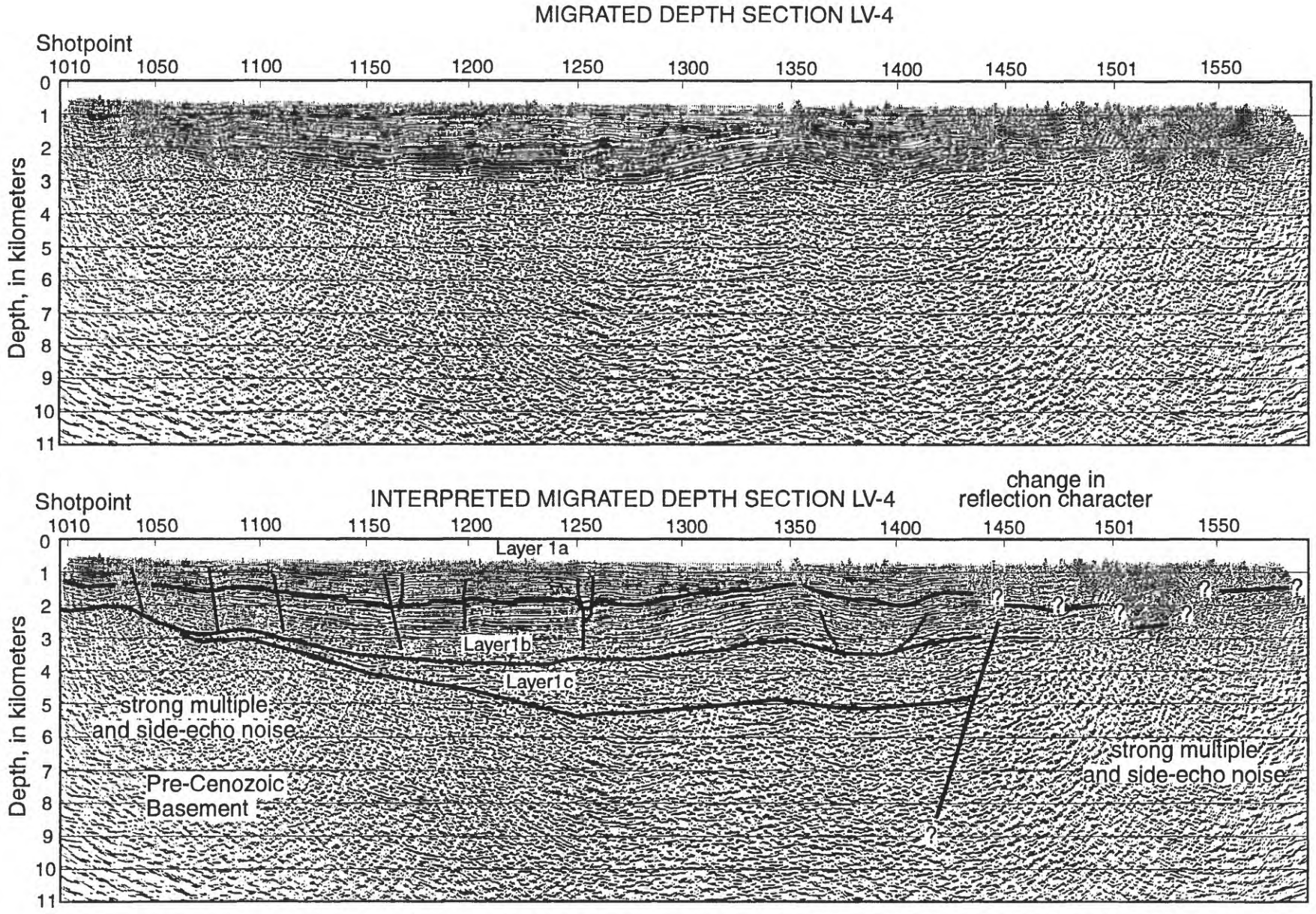

Figure 7. Uninterpreted and interpreted migrated depth sections along LV-4. Sea level is at +1 km depth. LV-4 is a non-exclusive profile purchased from Seitel Data, Inc. with limited publication rights. The profile was reprocessed by the U.S. Geological Survey.

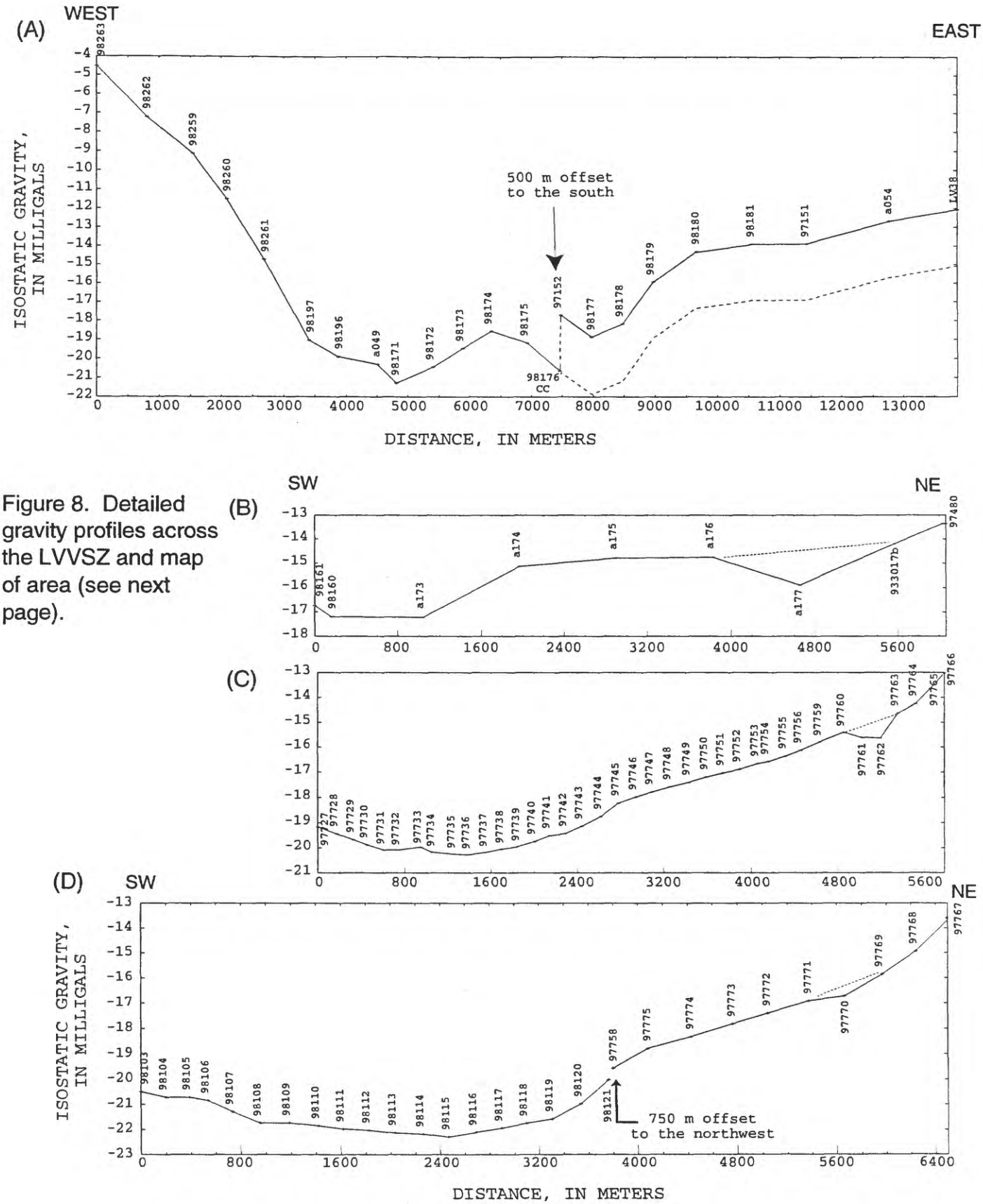

Figure 8. Detailed gravity profiles across the LVVSZ and map of area (see next page).

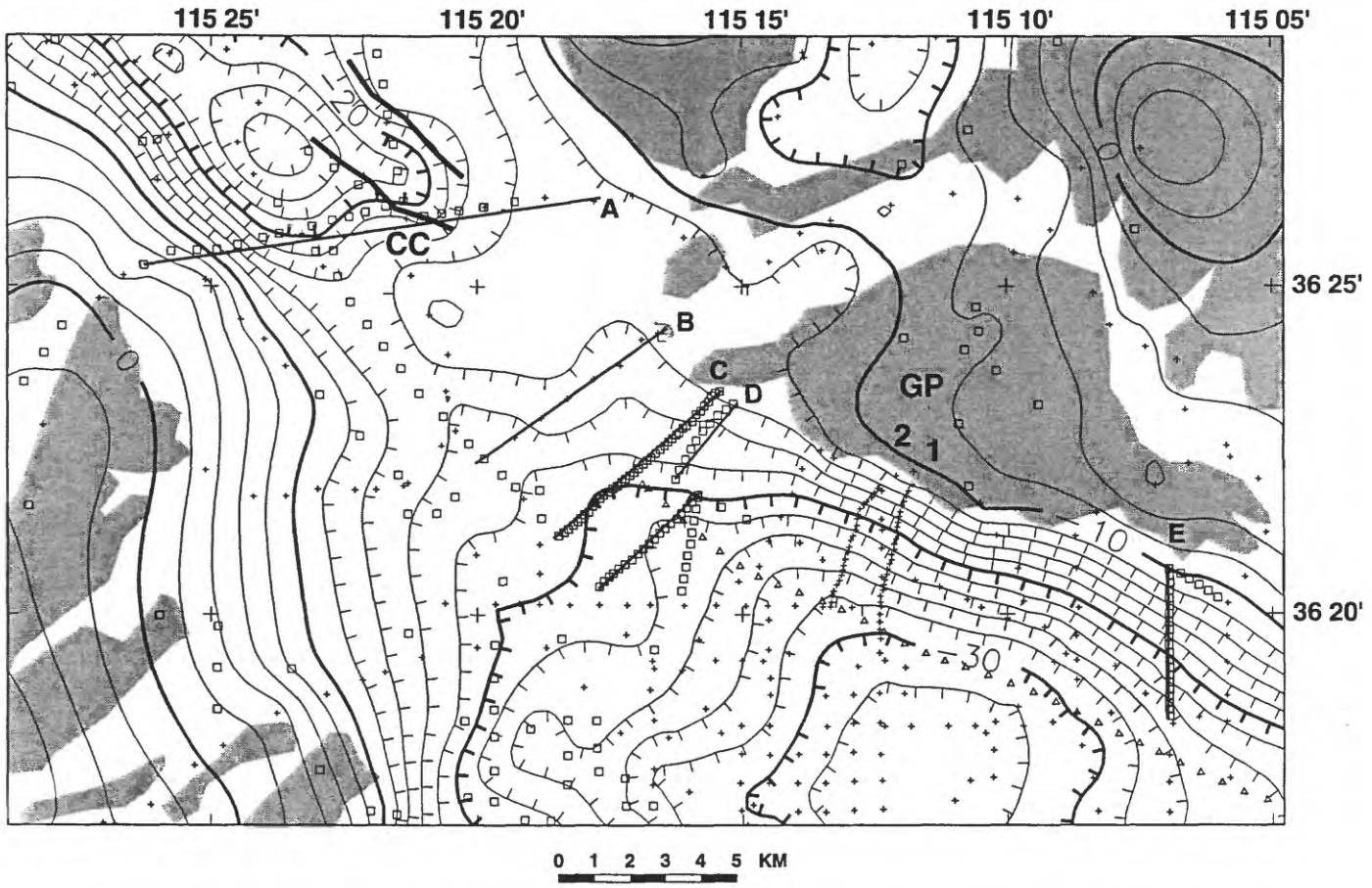

Figure 8. Isostatic gravity map showing detailed profiles across the LVVSZ. Contour interval 2 mGal. Boxes, new gravity stations; crosses, previous gravity stations. Thick black lines, faults from Quade (1986). Triangles are every 10th shot-point along LV-4. Detailed profiles are shown in panels (A) through (E). Profile A crosses through Corn Creek Springs (CC). Profile B consists mainly of previous stations. Note that profile A has a different horizontal and vertical scale than profiles B through E. Dotted lines on profiles B-D highlight local gravity lows discussed in text. GP, Gass Peak.

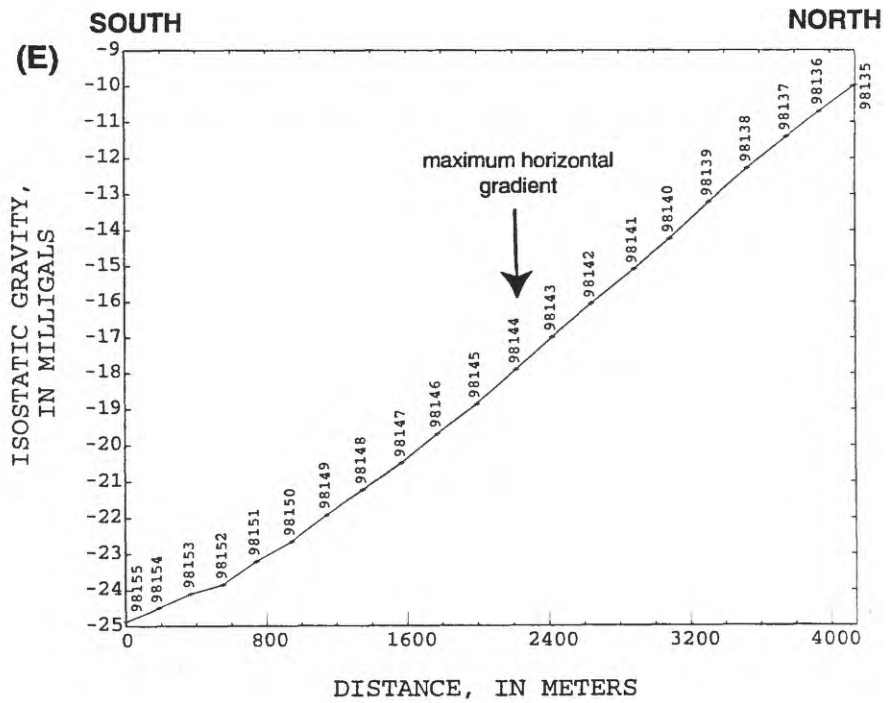

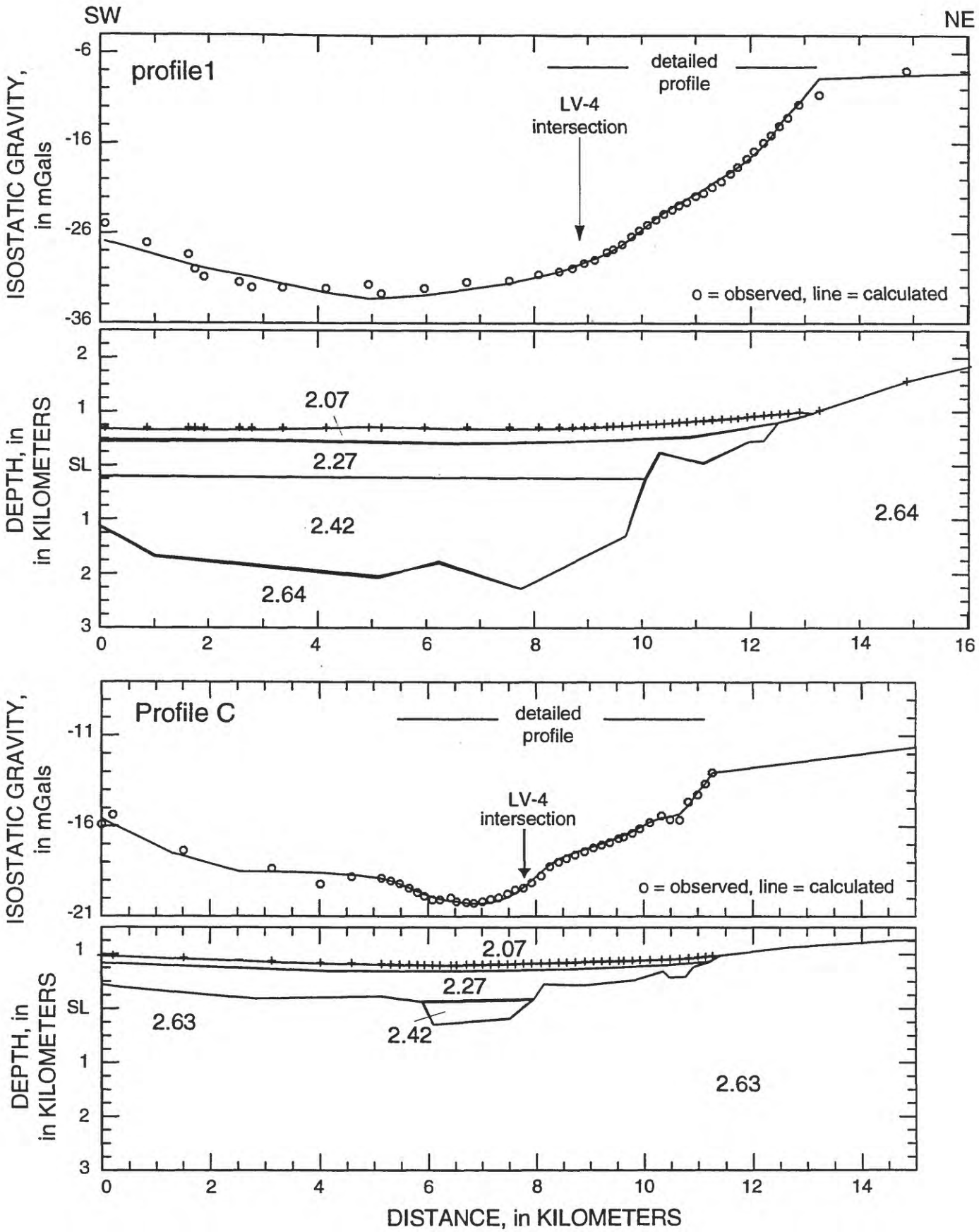

Figure 9. 2-1/2 dimensional gravity models along profiles 1 and C. See figure 8 for locations. Numbers in models are densities in g/cm^3.

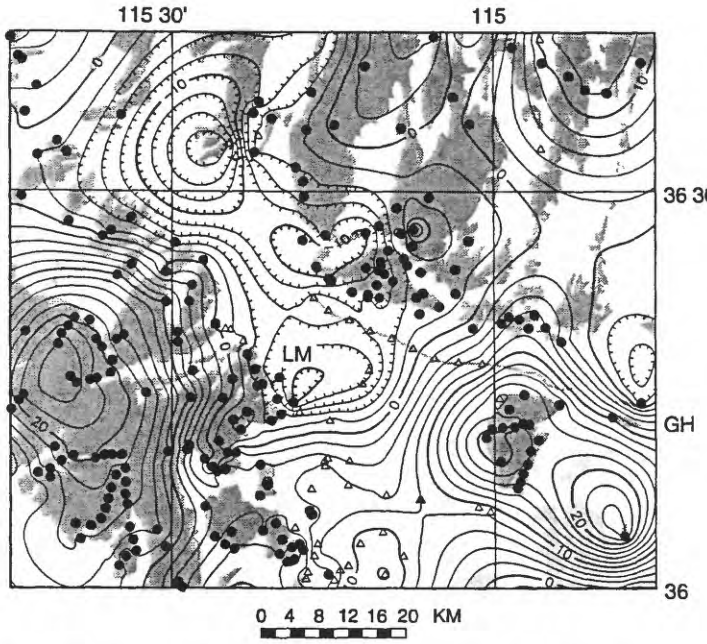

Well density-depth function and basement defined as base of Layer 1b

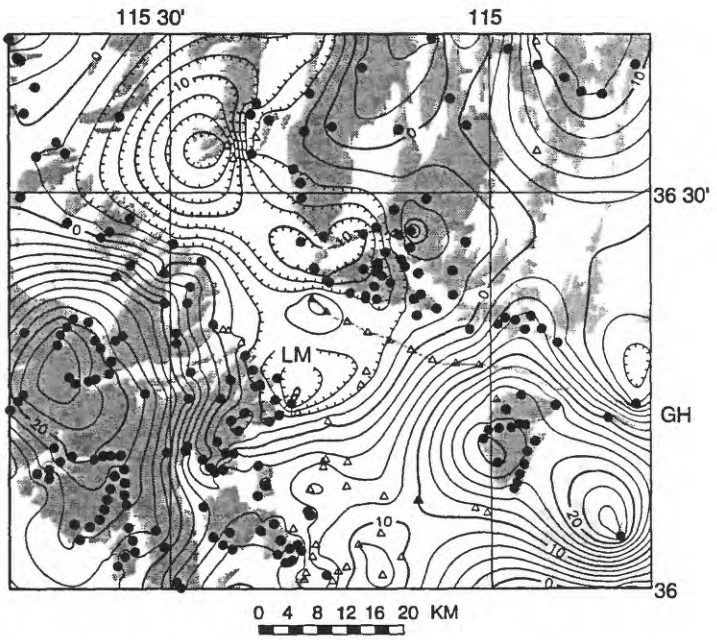

Seismic density-depth function and basement defined as base of Layer 1b

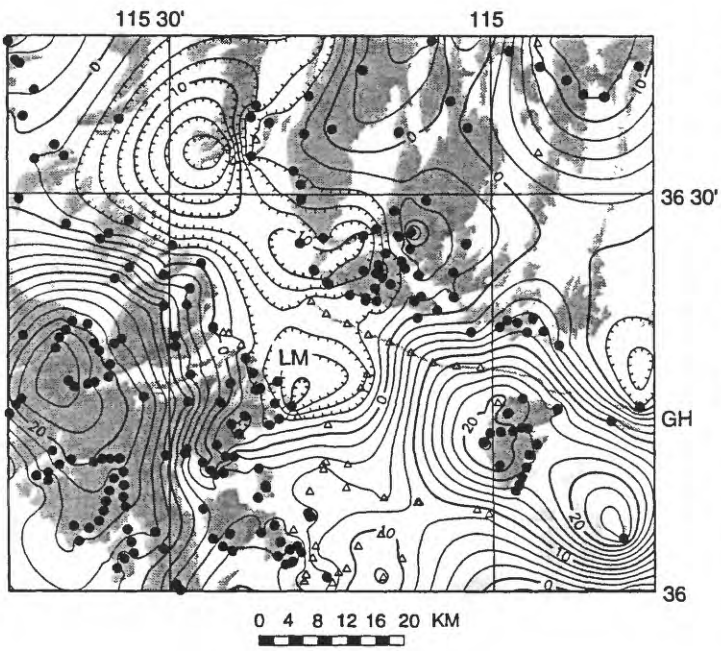

Well density-depth function and basement defined as base of Layer 1c

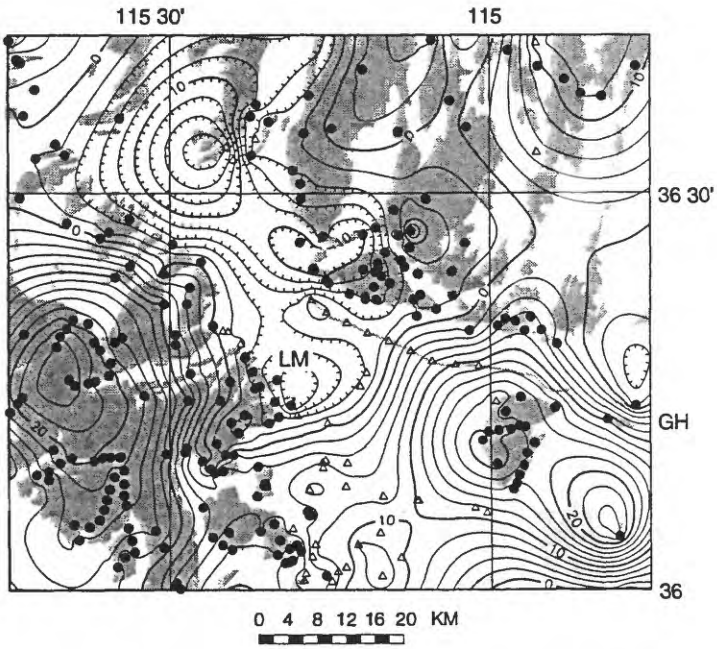

Seismic density-depth function and basement defined as base of Layer 1c

Figure 10. Basement gravity fields of the Las Vegas Valley shear zone region. Contour interval, 2mGal. Solid circles, gravity stations measured on basement; triangles, well and seismic picks on basement. Gray line is LV-4.

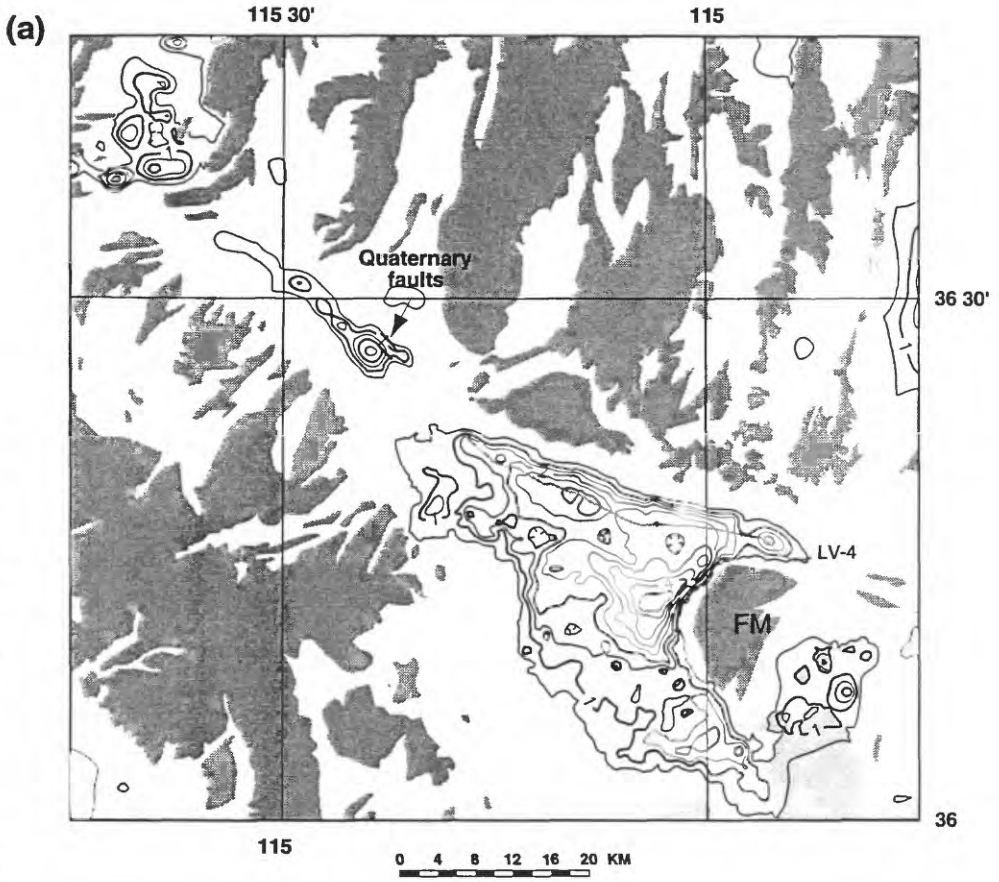

Figure 11. Thickness of Cenozoic rocks. See figure 2 for explanation of the geology. Contour intervals, 0.5 and 1.0 km. (a) Basin model using the well-derived density-depth function and picking the base of Layer 1b (Fig. 7) as the pre-Cenozoic surface. (b) Basin model using the seismic-derived density-depth function and picking the base of Layer 1c as the pre-Cenozoic surface.

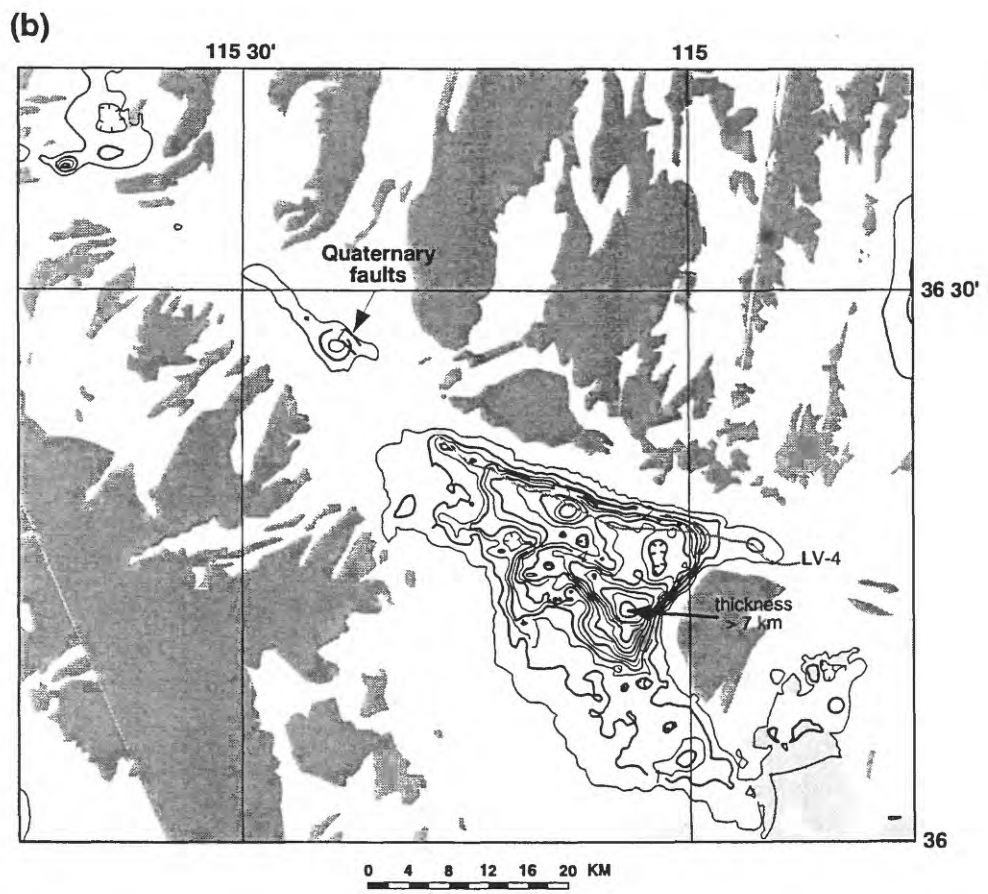

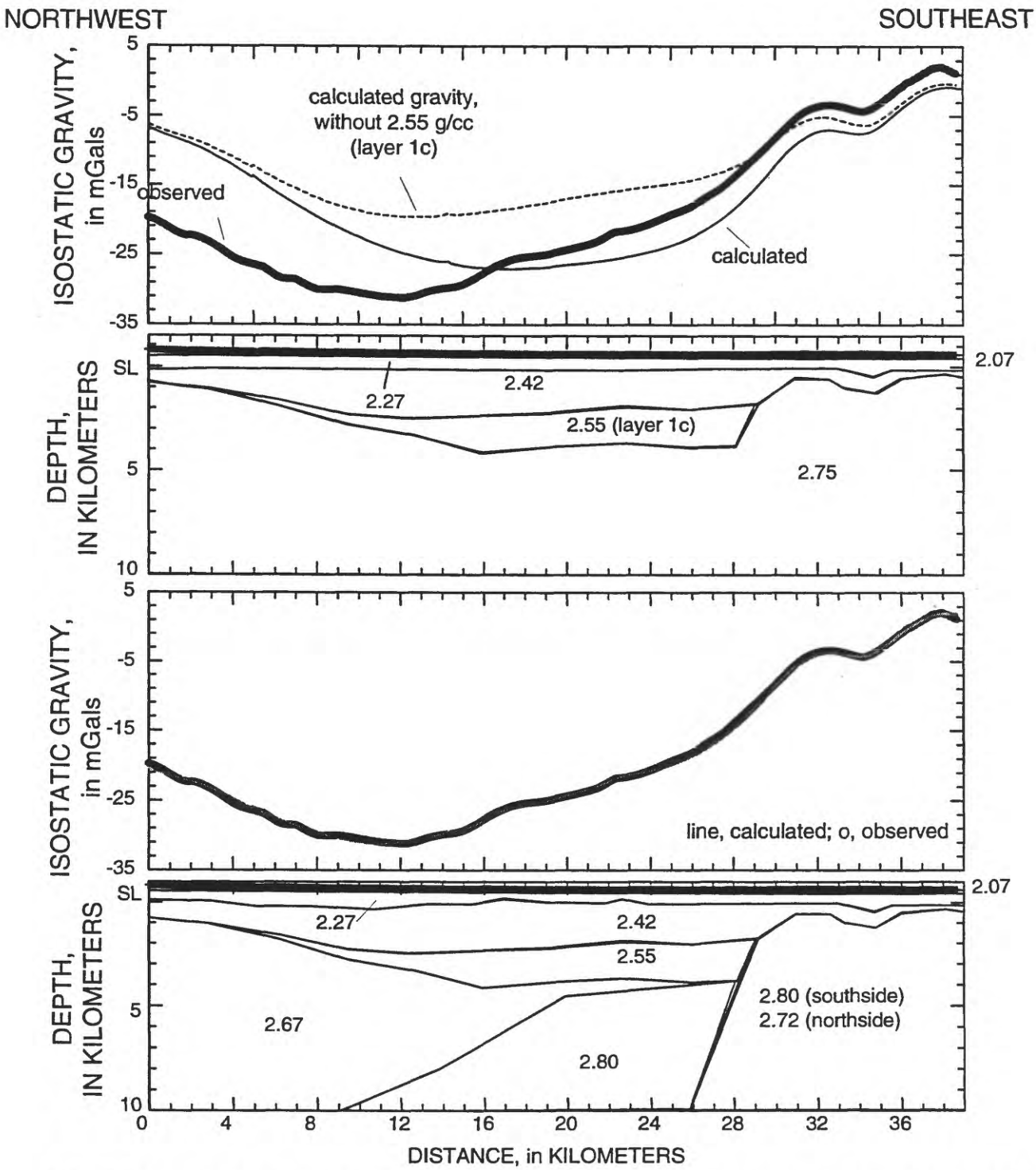

FIGURE 12. 2-1/2 dimensional gravity models along LV-4. Numbers on models are densities in g/cm3. Both models use the interpreted seismic picks for the base of layers 1b and 1c. A shows calculated gravity assuming no variations in basement density. B shows a possible solution. The geometry of the basement sources is not constrained. Aeromagnetic data were not modeled because LV-4 does not intersect magnetic source underlying Frenchman Mountain.